International Journal of Heat and Fluid Flow 72 (2018) 8–19

Contents lists available at ScienceDirect

International Journal of Heat and Fluid Flow

journal homepage: www.elsevier.com/locate/ijhff

Numerical parametric study of the evaporation rate of a liquid under a shear gas flow: Experimental validation and the importance of confinement on the convection cells and the evaporation rate

H. Machrafi[a,*], Y. Lyulin[b,c], C.S. Iorio[d], O. Kabov[b], P.C. Dauby[a]

[a] Université de Liège, Institut de Physique, B5a, Allée du 6 Août 19, Liège 1 B-4000, Belgium
[b] Institute of Thermophysics, Russian Academy of Sciences, Prosp. Lavrentyev 1, Novosibirsk 630090, Russia
[c] Novosibirsk State University, Pirogova Str. 2, Novosibirsk 630090, Russia
[d] Université libre de Bruxelles, Microgravity Research Center, Ecole Polytechnique, CP165/62, avenue F.D. Roosevelt, 50, Brussels 1050, Belgium

ARTICLE INFO

Keywords:
Evaporation
Shear flow
Confinement
Convection cell
Numerical modeling
Experimental validation

ABSTRACT

Evaporation can cause instability due to cooling effects on the density and surface tension. This causes, respectively, Rayleigh and Marangoni instabilities. When these instabilities grow sufficiently, self-sustained convection occurs. This convection causes changes into the evaporation rate and heat transfer rate. This also could change the heat transfer via the evaporation rate and can be important for industrial applications. It is the purpose of this paper to investigate the relation that exists between the overall evaporation rate and a set of parameters: temperature, gas flow and liquid thickness. Three-dimensional numerical simulations have been performed for this purpose and the results have been validated by means of an experimental setup, on which the numerical geometry has been based, characterized by a liquid evaporating through an opening in a cover sheet under a shear gas flow. It is shown that the temperature and the gas flow increase the evaporation rate. More interestingly, a maximum is observable for the evaporation rate as function of the liquid thickness. The explanation for these phenomena are drawn from the 3D numerical simulations. It appears that the maximum evaporation rate as a function of the liquid thickness depends on the confinement of the convection cells by the cover sheet, being assisted by the gas flow.

1. Introduction

Rayleigh-Bénard (RB), buoyancy-driven, and Marangoni-Bénard (MB), surface-tension-driven, convection of a fluid heated from below and/or cooled from above is a classical problem in fluid dynamics (e.g. Pearson, 1958; Bénard, 1901; Norman et al., 1977; Colinet et al., 2001). It played a crucial role in the development of stability theory in hydrodynamics (Chandrasekhar, 1981; Drazin and Reid, 1981) and had been paradigmatic in pattern formation and in the study of spatial-temporal chaos (Getling, 1998; Bodenschatz et al., 2000). RB and MB convection also play important roles in recent stability analyses where evaporation is the driving force (Haut and Colinet, 2005; Bestehorn, 2007; Machrafi et al., 2011; Machrafi et al., 2013a). From an applied viewpoint, thermally driven flows are of utmost importance. A non-exhaustive list of examples comprises thermal convection in the atmosphere, in oceans, buildings, process technology. These thermal flows can give rise to certain self-sustained patterns that can be stationary or can change into other patterns or even to chaotic structures. We are here especially interested in evaporation-related thermal flows. These have been studied theoretically, numerically and experimentally, e.g. Bestehorn and Merkt (2006), Iorio et al. (2011), Lyulin and Kabov (2014) and Machrafi et al. (2014), to mention a few. This work falls into a general framework which consists of observing the behavior of the evaporation rates as a function of a set of parameters: the temperature, the gas flow and the liquid thickness. In previous work, such a configuration has been studied with regard to theoretical instability thresholds (Machrafi et al., 2013b). What is of interest here, is a three-dimensional numerical simulation of the temperature and fluid motion in the liquid for a liquid evaporating into a horizontal nitrogen gas flow. The chosen liquid is HFE7100 (an electronics coolant liquid produced by 3 M). The numerical simulations (CFD) are performed using the software ComSol (finite elements method). The numerical results are validated experimentally, using an experimental setup (Lyulin and Kabov, 2014), on which the numerical simulation geometry is based. The evaporation, taking place at the upper surface of the liquid layer results into the cooling of the liquid surface. This cooling induces

* Corresponding author.
E-mail address: h.machrafi@uliege.be (H. Machrafi).

https://doi.org/10.1016/j.ijheatfluidflow.2018.05.003
Received 16 May 2017; Received in revised form 28 November 2017; Accepted 4 May 2018
0142-727X/ © 2018 Elsevier Inc. All rights reserved.

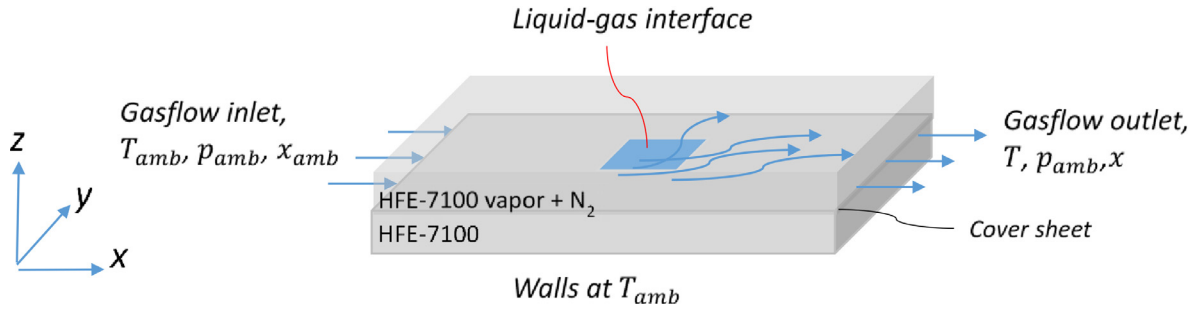

Fig. 1. The schematic of the physical system.

temperature gradients in the liquid. These temperature gradients are in turn responsible for the development of a thermal boundary layer that develops from the liquid-gas interface into the bulk liquid. Since density and surface tension depend both on the temperature, the temperature gradients cause them to change. As a consequence, locally colder zones of fluid will have a higher density and surface tension than their neighboring fluid particles, which will cause the fluid to move. When the thermal gradient exceeds a certain threshold, instability sets in and self-sustained convective patterns take place. As time proceeds, these patterns can become chaotic. The numerical setup in the present work is based on a so-called evaporator, which takes part of a pre-flight analysis of the EVAPORATION PATTERNS (EP) (previously named CIMEX) experimental setup of the European Space Agency (ESA), to be flown aboard a satellite in the near future. A sketch of the physical system is presented in Fig. 1.

The physical setup that will be numerically studied has overall dimensions of 50 mm by 50 mm with a certain liquid height, h_{liq}, variable from 1.5 mm to 8 mm. The evaporated liquid is considered to be constantly replenished from the bottom, so that the gas-liquid interface, present within an opening 10.6 mm by 10.6 mm, remains at the same level. Evaporation is allowed through this opening, while gas absorption into the liquid is neglected. Above it, there is a gas channel with a height, h_{gas}, of 5 mm and a width of 50 mm. In this channel, nitrogen is injected with flow rates, Q_{gas}, between 100 and 5000 ml/min. The gas flow at the gas channel entrance has a certain imposed relative humidity η in HFE-7100 vapor in nitrogen. The relative humidity can be varied from 0% to 100%, expressed in an ambient (denoted by the subscript "*amb*") molar fraction x_{amb} via the relation $x_{amb} \equiv \eta p_{sat}(T_{amb})/p_{amb}$, where p_{sat} is the saturation pressure of the vapor, while T_{amb} is an ambient temperature between 20 and 40 °C and p_{amb} an ambient pressure of 1 atm. At the exit, we have an open boundary with a constant pressure, where the molar fraction satisfies a zero-flux condition (meaning that we assume that after the exit the molar fraction does not change, which is approximately the case in the EP experiment). Between the gas and liquid layers a cover sheet is placed to separate them, except for an assumed undeformable 10.6 mm-square opening. The rest of the interfaces of the system are walls kept at a constant temperature T_{amb}. One of the goals of this EP experiment is to quantify mass-transfer processes across interfaces, i.e. evaporation, and their coupling with surface-tension-driven (Marangoni) and density-driven (Rayleigh) flows/convection in a liquid. In this work, we focus on presenting a parametric study of such convection, in order to analyze specific behavior of the evaporation process as a function of those parameters. Particular attention is given to the effect of the liquid layer thickness, which takes into consideration the effect confinement by the cover can have on the number of convection cells and its result on the evaporation rate. The paper is organized as follows. Section 2 provides a mathematical description of the model with the boundary conditions. Section 3 deals with the numerical part as well as the experimental setup used for validating the numerical results. Section 4 shows the results, followed by the conclusions in Section 5.

2. Model

The Boussinesq approximation is adopted for both phases of the system, implying that the material properties of the fluids are treated as constant except for the density in the buoyancy terms, where it depends linearly on the temperature and the molar fraction, and the surface tension in the stress balance at the interface, where it depends linearly on the temperature. Before starting with the equations in the bulk and the boundary conditions, we provide the expressions for the density as used in the buoyancy terms (under the Boussinesq approximation):

$$\tilde{\rho}_l = \rho_l(1 - \alpha_l(T_l - T_{l,0})) \tag{1}$$

$$\tilde{\rho}_g = \rho_g(1 - \alpha_g(T_g - T_{g,0}) - \varepsilon_g(\chi_g - \chi_{g,0})) \tag{2}$$

In (1) and (2), ρ is the density (the tilde denotes the density under the Boussinesq approximation), α and ε denote the thermal and the solutal expansion coefficients. The subscripts "l" and "g" relate to the liquid and gas phases, respectively. The subscript "0″ refers to a state with a certain typical value of the temperatures and molar fraction, here taken to be $T_{l,0} = T_{g,0} = T_{amb}$ and $\chi_{g,0} = \chi_{amb}$. The densities ρ_l and ρ_g are taken at ambient conditions.

The equations for the bulk, in both the gas and liquid phases, are then given by

$$\nabla \cdot \vec{v_l} = 0, \tag{3}$$

$$\rho_l \frac{\partial \vec{v_l}}{\partial t} = -\rho_l \left(\vec{v_l} \cdot \vec{\nabla}\right)\vec{v_l} - \vec{\nabla} p_l + \mu_l \nabla^2 \vec{v_l} + \rho_l(1 - \alpha_l(T_l - T_{l,0}))\vec{g}, \tag{4}$$

$$\frac{\partial T_l}{\partial t} = -\left(\vec{v_l} \cdot \vec{\nabla}\right) T_l + \kappa_l \nabla^2 T_l, \tag{5}$$

$$\nabla \cdot \vec{v_g} = 0, \tag{6}$$

$$\rho_g \frac{\partial \vec{v_g}}{\partial t} = -\rho_g \left(\vec{v_g} \cdot \vec{\nabla}\right)\vec{v_g} - \vec{\nabla} p_g + \mu_g \nabla^2 \vec{v_g} + \rho_g(1 - \alpha_g(T_g - T_{g,0}) - \varepsilon_g(\chi_g - \chi_{g,0}))\vec{g}, \tag{7}$$

$$\frac{\partial T_g}{\partial t} = -\left(\vec{v_g} \cdot \vec{\nabla}\right) T_g + \kappa_g \nabla^2 T_g, \tag{8}$$

$$\frac{\partial \chi_g}{\partial t} = -\left(\vec{v_g} \cdot \vec{\nabla}\right) \chi_g + D_g \nabla^2 \chi_g, \tag{9}$$

where $\vec{v}$ and p are the (barycentric) velocity and pressure fields, respectively. Furthermore, D_g is the diffusion coefficient of HFE vapor in N_2 and μ the dynamic viscosity. Note that the thermal diffusivity κ is also defined by $\kappa = \lambda\, \rho^{-1} c_p^{-1}$, with λ and c_p being the thermal conductivity and heat capacity, respectively. For the liquid and gas phases respectively, (3) and (6) are the continuity equations for incompressible fluids, (4) and (7) are the momentum equations, (5) and (8) express the energy conservation, whereas (9) stands for the species conservation in the gas phase. The last terms of Eqs. (4) and (7), respectively, represent

Download English Version:

https://daneshyari.com/en/article/7053423

Download Persian Version:

https://daneshyari.com/article/7053423

Daneshyari.com